

# 2 PF Ring

## 2-1 Operation Summary

The timetable of machine operation in FY2008 and the operation statistics are summarized in Fig. 1 and Table 1, respectively. Total operation time, scheduled user time, actual user time, wiggler operation time, and single-bunch user time in each fiscal year since the commencement of the operation are illustrated in Fig. 2. The total operation time was recovered after the straight-section upgrade project in 2005, amounting to more than 5000 h for each of the past three years. However, the operation time gradually decreases year after year with the reduction of the operation budget. In FY2008, the scheduled user time and the actual user time excluding the time losses due to machine trouble and daily injections were 4032.0 and 3943.6 h, respectively. The ratio of the actual user time to the scheduled time has been maintained at 96%–98% for the past seven years. Figure 3 shows the product  $I\tau$  of the beam current  $I$  and the beam lifetime  $\tau$  over the past 12 years. The  $I\tau$  gradually recovered after the reconstruction for the straight-section upgrade project, while it rapidly decreased in the spring of 2006 and in the spring of 2007. The decreases in the  $I\tau$  in FY2006 and FY2007 were due to vacuum troubles with SR absorbers. Figure 4

shows the average stored beam current and the injection interval since 1982. Although the injection frequencies in 2004 and 2005 were twice a day, it was restored to once a day in FY2007. The failure rate, which is the ratio of the failure time to the total operation time, is shown in Fig. 5. Although the rate was around 1% throughout the 1990s, it has been improved to around 0.5% over the past several years. However, the rates of 0.85% in FY2006, 1.8% in FY2007, and 0.83% in FY2008 were considerably large; this was due to the problems related to SR absorber troubles and so on.

In FY2008, the initial beam current was maintained at 450 mA in the multibunch mode at a beam energy of 2.5 GeV. Beam injection was carried out with the main beam shutters kept open, and the injection frequency was increased to twice per day. For optional operations, the ring was operated for one week with beam energy of 3.0 GeV in the multibunch mode. During the operation at 3.0 GeV, the stored beam current was limited to less than 200 mA in consideration of the heat load and the radiation safety for the beamlines. In addition, the operation in the single-bunch mode with beam energy of 2.5 GeV was conducted twice. (During the operation in the single-bunch mode, the stored beam current was generally maintained at 50 mA with top-up injections.)

Table 1 Operation statistics of PF ring in FY2008.

	Multi-bunch	Single-bunch	Total
Ring Operation Time (hours)	4712.0	288.0	5000.0
Scheduled user time (hours)	3744.0	288.0	4032.0
Actual user time T (hours)	3663.2	280.3	3943.6
Time used for injection (hours)	45.8	1.3	47.1
Integrated current in T (A×hours)	1347.3	13.7	1361.0
Average current in T (mA)	367.8	48.8	--
Number of injections	321	Top-up	--
Interval between injections (hours)	11.4		--

	SUN	MON	TUE	WED	THU	FRI	SAT	SUN	MON	TUE	WED	THU	FRI	SAT	SUN	MON	TUE	WED	THU	FRI	SAT
	9 17	9 17	9 17	9 17	9 17	9 17	9 17	9 17	9 17	9 17	9 17	9 17	9 17	9 17	9 17	9 17	9 17	9 17	9 17	9 17	9 17
Date	4.13	14	15	16	17	18	19	20	21	22	23	24	25	26	27	28	29	30	5.1	2	3
PF																					
AR																					
Date	4	5	6	7	8	9	10	11	12	13	14	15	16	17	18	19	20	21	22	23	24
PF																					
AR																					
Date	25	26	27	28	29	30	31	6.1	2	3	4	5	6	7	8	9	10	11	12	13	14
PF																					
AR																					
Date	15	16	17	18	19	20	21	22	23	24	25	26	27	28	29	30	7.1	2	3	4	5
PF																					
AR																					
Date	9.28	29	30	10.1	2	3	4	5	6	7	8	9	10	11	12	13	14	15	16	17	18
PF																					
AR																					
Date	19	20	21	22	23	24	25	26	27	28	29	30	31	11.1	2	3	4	5	6	7	8
PF																					
AR																					
Date	9	10	11	12	13	14	15	16	17	18	19	20	21	22	23	24	25	26	27	28	29
PF																					
AR																					
Date	30	12.1	2	3	4	5	6	7	8	9	10	11	12	13	14	15	16	17	18	19	20
PF																					
AR																					
Date	21	22	23	24	25	26	27	28													
PF																					
AR																					
Date	1.11	12	13	14	15	16	17	18	19	20	21	22	23	24	25	26	27	28	29	30	31
PF																					
AR																					
Date	2.1	2	3	4	5	6	7	8	9	10	11	12	13	14	15	16	17	18	19	20	21
PF																					
AR																					
Date	22	23	24	25	26	27	28	3.1	2	3	4	5	6	7	8	9	10	11	12	13	14
PF																					
AR																					
Date	15	16	17	18	19	20	21	22	23	24	25	26	27	28	29	30	31	4.1	2	3	4
PF																					
AR																					

PF: PF ring  
AR: PF-AR

- Tuning and ring machine study
- Short maintenance and /or machine study
- Ring machine study
- Experiment using SR
- Single bunch operation at 2.5 GeV
- Multi bunch operation at 3.0 GeV

Note) "B\*" in the table is a bonus time that the ring has the priority.

Figure 1  
Timetable of machine operation in FY2008.

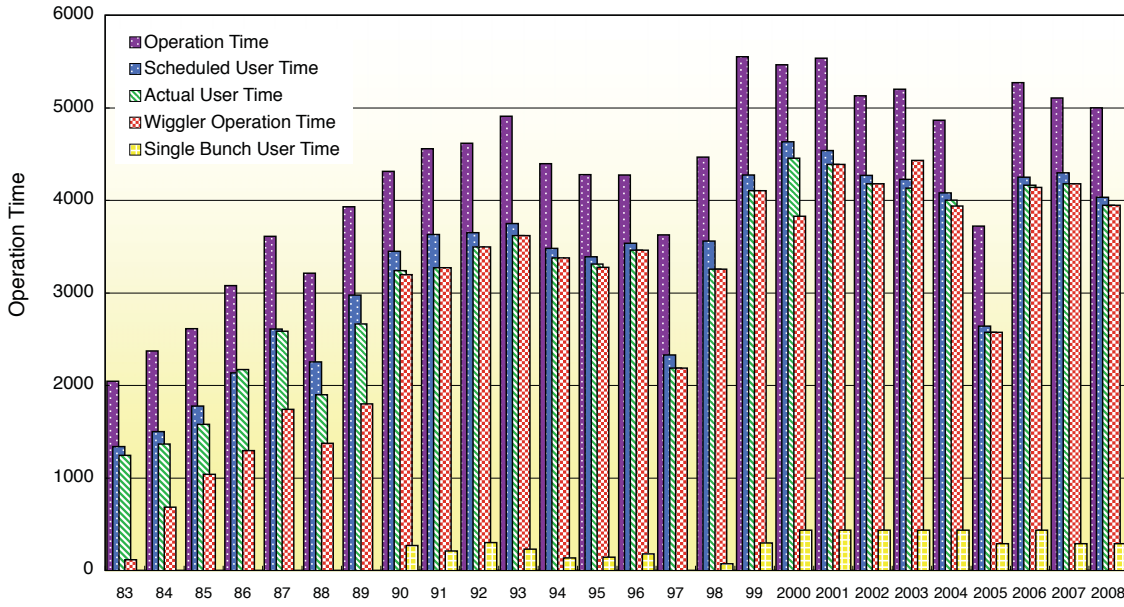


Figure 2 Total operation time, scheduled user time, actual user time, wiggler operation time, and single-bunch user time in each fiscal year since the commencement of the operation.

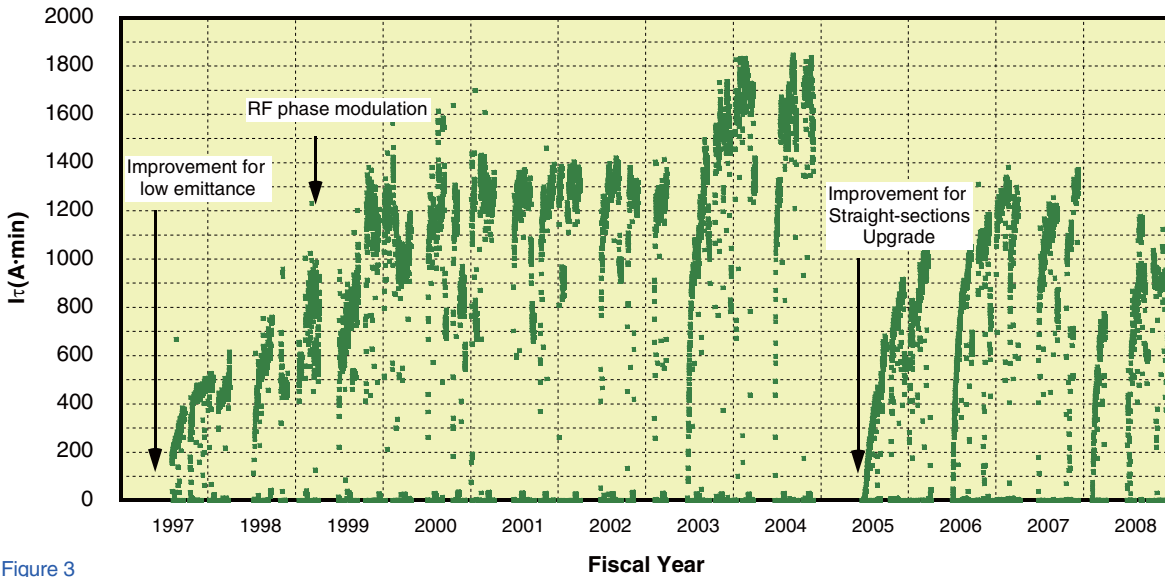


Figure 3 Product  $I\tau$  of the beam current  $I$  and the beam lifetime  $\tau$  for the past 12 years.

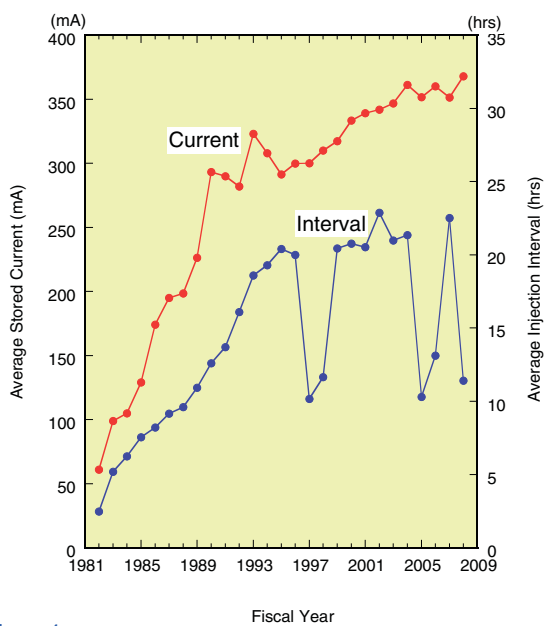


Figure 4 Average stored beam current and injection interval.

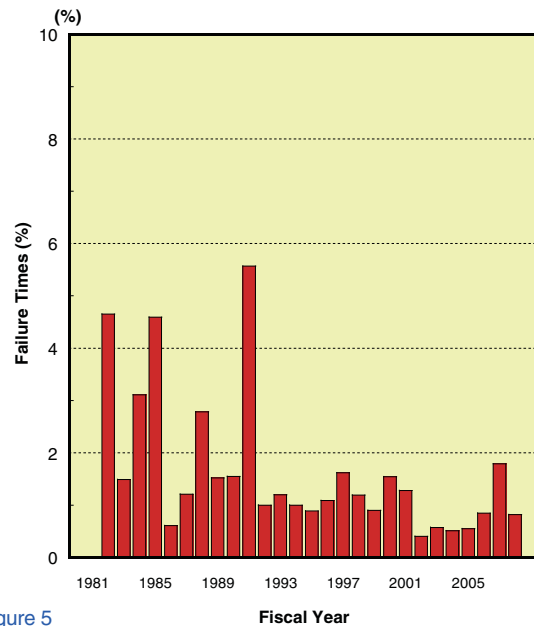


Figure 5 Failure rate, which is the ratio of the failure time to the total operation time.

## 2-2 Injector Linac Upgrade for PF Ring in Top-Up Injection Mode

The KEK injector linac sequentially generates beams in different modes and transfers them to the following four storage rings: KEKB low-energy ring (LER) (3.5 GeV/positron), KEKB high-energy ring (HER) (8 GeV/electron), Photon Factory ring (PF ring; 2.5 GeV/electron), and Advanced Ring for Pulse X-rays (PF-AR; 3 GeV/electron). Beam injection to the PF ring and PF-AR is carried out twice a day, whereas the KEKB rings are operated in the continuous injection mode (CIM) so that the stored current remains almost constant. The KEK Linac upgrade project has been in progress since 2004 so that the PF top-up and KEKB CIM can be performed at the same time. The aim of this upgrade project is to change the linac parameters (beam mode) up to 50 Hz (in 20-ms intervals), which is the maximum linac beam repetition rate, by using a multienergy linac scheme. In this scheme, common DC magnet settings are used for the KEKB and PF rings. The beam energy is adjusted in a pulse-to-pulse manner by rapid control of a low-level RF phase.

A positron production target with a hole is used to enable rapid switching between the positron and electron modes. The target is 14 mm thick and is made of amorphous tungsten. Recently, a 10-mm-thick crystal tungsten target has been designed for practical applications; when using this target, a 25% increase in the positron intensity is observed [1]. The transverse cross section of the crystal tungsten target is a square of side 4.5 mm. The target is combined in a copper support by hot isostatic pressing. The primary electron beam hits the target in the positron mode. In the electron mode, the primary electron beam is kicked by pulsed steering magnets and made to pass through the hole.

For the linac upgrade, it is necessary to carry out fast measurements of the beam position. When the beam is simultaneously operated in the PF top-up injection mode and KEKB CIM, every beam position should be measured up to 50 Hz. Hence, we have developed a new data acquisition (DAQ) system for beam position monitoring [2]. In the KEK linac, approximately 90 stripline beam position monitors (BPMs) have been installed for carrying out nondestructive measurements and for feedback. The 19 old BPM-DAQ systems, each of which consist of a VME and a digital oscilloscope (Tektronix TDS680B), have been replaced by 23 new DAQ systems, each of which comprises a fast digital oscilloscope (Tektronix DPO7104). This digital oscilloscope is WindowsXP based and is equipped with a 3.4 GHz Pentium-IV microprocessor; it provides a sampling rate of 10 GSa/s. With the new system, the rate of repetitive waveform acquisition can be made to exceed 120 Hz with a 20-k data-point length; this rate is sufficient for 50-Hz beam position measurements. We have also developed a new DAQ software that functions as an EPICS IOC and as a high-level application for orbit display. This system functions stably during daily operations.

Towards to the complex beam operation in the simultaneous injection, the importance of the safety system also increases. For this reason, a new PLC-based beam-charge interlock system has been developed for radiation safety [3]. This system controls the integrated beam charge at various locations to ensure machine protection and monitors the amount of integrated beam charge delivered to the four storage rings in the linac beam switchyard. The charge of the electron beams delivered from an electron gun is measured by the beam-charge interlock system, which consists of wall current monitors, beam-charge integration circuits and a PLC-

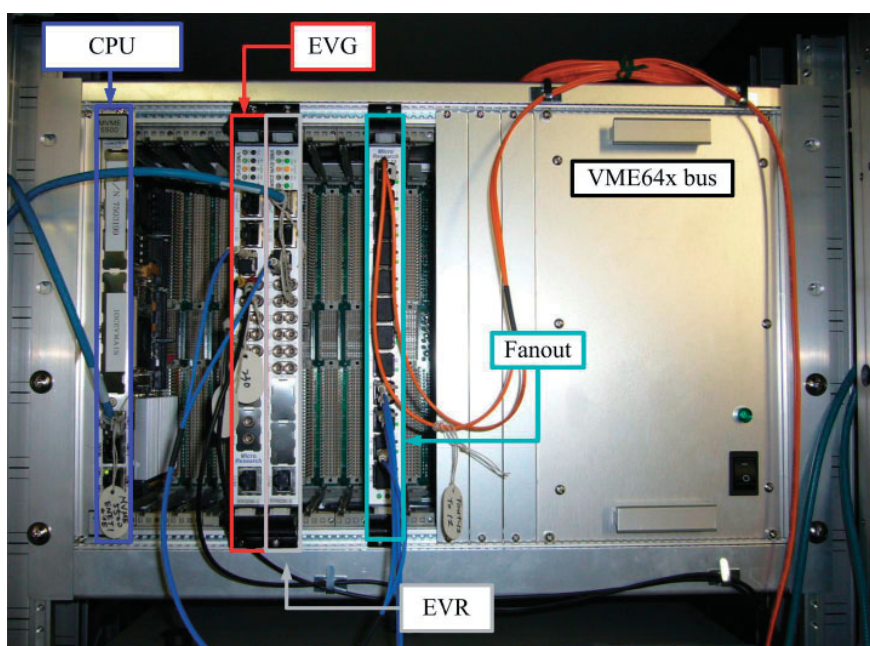


Figure 6  
New timing system.

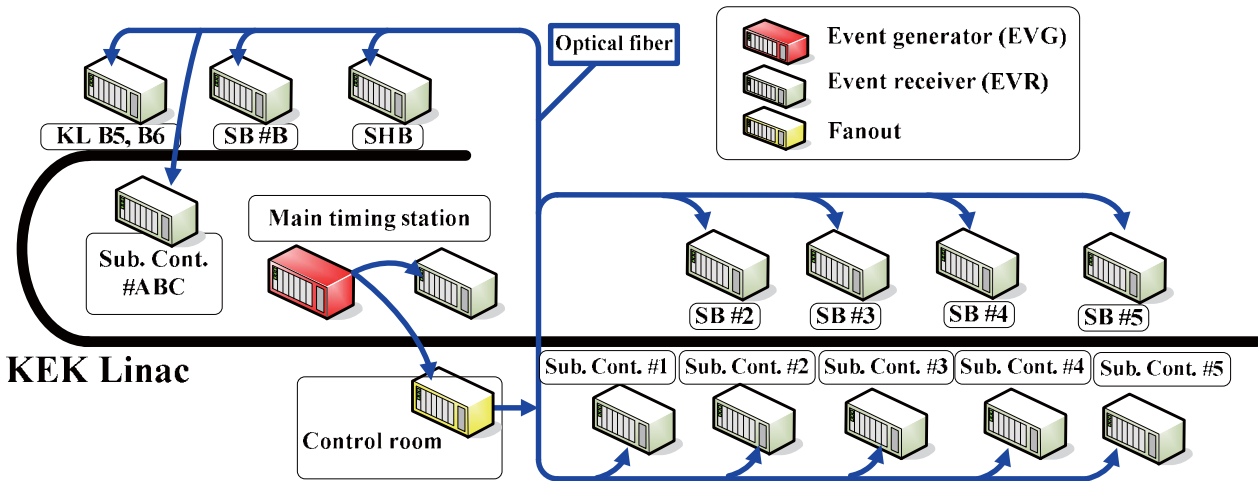


Figure 7  
Beam operation using one EVR and a set of fourteen EVRs.

based control system. When the amount of integrated beam charge exceeds the prescribed threshold level, this system sends beam abort signals directly to another radiation safety system via hardwired cables. This system has been used in daily operations of the linac.

When upgrading the KEK linac, it is also indispensable to upgrade the timing system. In the old timing system, approximately 150 time delay modules based on a VME bus (TD4V) and CAMAC (TD4) were used for controlling the timing signals distributed to different types of local controllers at different locations. An event generator and receiver (EVG/EVR) system based on a VME64x bus is adopted as the new timing system, as shown in Fig. 6. Using this system, event information (beam mode), RF clock (114 MHz), timestamp values, and data buffers can be rapidly transferred from the EVG to the EVR via optical fibers. Some of the VME crates include DAC/ADC boards for controlling and monitoring the low-level RF phase. Beam operations have been carried out using one EVR as well as a set of fourteen EVRs, as shown in Fig. 7. We have also developed an operation software based on the EPICS system. Figure 8 shows the image of a control panel used in the new timing system. The operators can easily generate any beam mode pattern. The new timing system is also utilized for daily operations of the linac, and three additional EVGs will be installed during the summer shutdown in 2009.

During the shutdown period (January to March, 2009) at KEKB, beam studies were carried out for identifying the available beam operation parameters for the multienergy linac scheme [5]. Using these operation parameters, a test operation aimed at simultaneous top-up injection to the PF and KEKB rings will be carried out in early FY2009. Operations involving the PF top-up in the KEKB CIM have been planned for execution in autumn 2009.



Figure 8  
Example of control panel used in the new timing system.

REFERENCES

- [1] T. Suwada, M. Satoh, K. Furukawa, T. Kamitani, T. Sugimura, K. Umemori, H. Okuno, Y. Endou, T. Haruna, R. Hamatsu, T. Sumiyoshi, K. Yoshida, A. P. Potylitsyn, I. S. Tropin and R. Chehab, *Phys. Rev. ST Accel. Beams*, **10** (2007) 073501.
- [2] M. Satoh, T. Suwada, K. Furukawa, J. Wang, T. Kudou, S. Kusano, *Proc. of ICALEPCS 2007*, (2007) 469.
- [3] T. Suwada, E. Kadokura, M. Satoh and K. Furukawa, *Review of Scientific Instruments*, **79** (2008) 023302.
- [4] K. Furukawa, M. Satoh, T. Suwada, T. Kudou, S. Kusano, A. Kazakov, G. Lei and G. Xu, *Proc. of LINAC 2008*, (2008) 404.
- [5] Y. Ohnishi, T. Kamitani, N. Iida, M. Kikuchi, K. Furukawa, M. Satoh, K. Yokoyama and Y. Ogawa, *Proc. of LINAC 2008*, (2008) 413.



## 2-3 Operation of an Elliptically Polarizing Undulator

An elliptically polarizing undulator (EPU), U#16-1, was constructed and installed into the ring in April 2008. Figures 9 (a) and (b) show the photographs of U#16-1 and the vacuum chamber, respectively, at the straight section of BL15-16. U#16-1 and a forthcoming identical undulator (U#16-2) comprise a polarization-switching source with a fast kicker system. U#16-1 has four variable rows of magnetic arrays to change the polarization states and a mechanism of gap driving to change the photon energy. The typical operation modes are composed of a symmetric and an antisymmetric mode. In the symmetric mode, we displace one pair of rows opposing diagonally to the other diagonal pair. The symmetric mode plays a major role in obtaining various polarization states that are obtained by (1) rotating the polarization angle from the horizontal to the vertical direction in case of linear polarization and (2) left or right rotation in case of circular or the elliptical polarizations.

In the antisymmetric mode, we can obtain the linear polarization with an arbitrary polarization angle, which can be rotated from the horizontal to the vertical direction in the linear polarization state.

By moving the four rows of magnetic arrays individually, we can use U#16-1 as both the usual APPLE-II type EPU and the adjustable phase undulator (APU). In APU, we move the top pair of the magnetic rows longi-

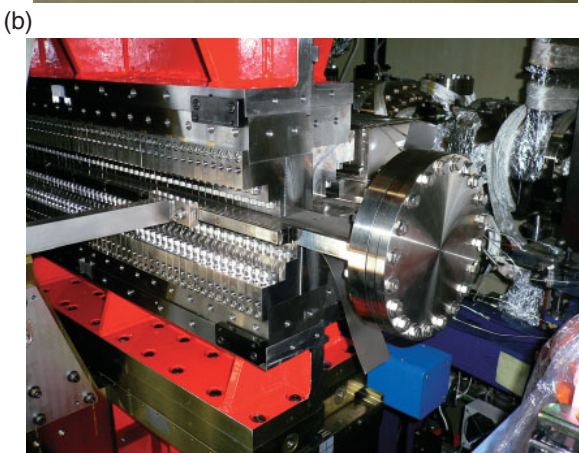
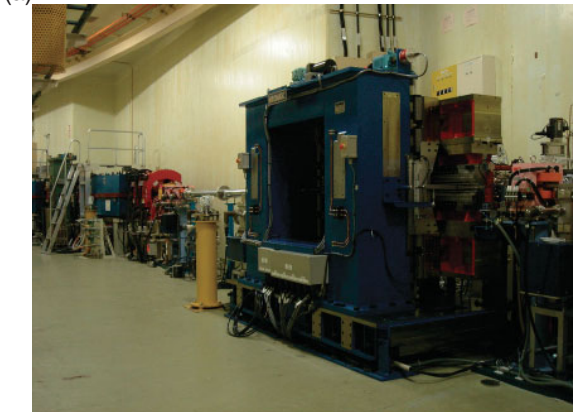


Figure 9  
(a) Photograph of U#16-1. (b) Photograph of the vacuum chamber of U#16-1.

tudinally with respect to the bottom pair; however, the gap is fixed to change the photon energy. The operation was started in the APU mode for the user experiments to tune both the energy and the polarization by adjusting the longitudinal position of all the four rows.

### (a) Operation for the user experiments

The operation of U#16-1 was successfully begun in May 2008 for user experiments in the circular polarization mode. Until the installation of U#16-2, the photon energy and the direction of polarization have to be changed frequently to satisfy the demand of experiments by the single operation of U#16-1. Hence, we adopted the APU mode to tune the photon energy by changing the pair phase with fixed gap of 21 mm since the closed orbit distortion (COD) and the tune shift are smaller compared to the gap change. Then, we can correct the COD easily by using steering magnets located at both ends of the undulator; the control system is simple and can be used to tune the photon energy and the polarization states.

The commissioning of U#16-1 in the APU mode was gradually achieved in the symmetric mode with various polarization states. At present, the available polarization modes are circular polarization ( $B_x/B_y = 1$ ), elliptical polarization ( $B_x/B_y = 1/2$ ), and linear polarization along the horizontal and vertical directions. We can change the row or the pair phase of U#16-1 in these modes at any time during the operation without disturbing the electron orbit.

### (b) Spectrum of U#16-1 in APU mode

In the first operation of U#16-1 after commissioning, it was used as a circular polarized source of the APU mode. The measured spectra have different features compared to the usual EPU mode in which the photon energy is controlled by the combination of the gap and the row phase. Figure 10 shows the obtained spectra in the case of circular polarization in the APU and EPU modes. The intensity of photon flux decreases by 50%, and the bandwidth of the first harmonic peak increases

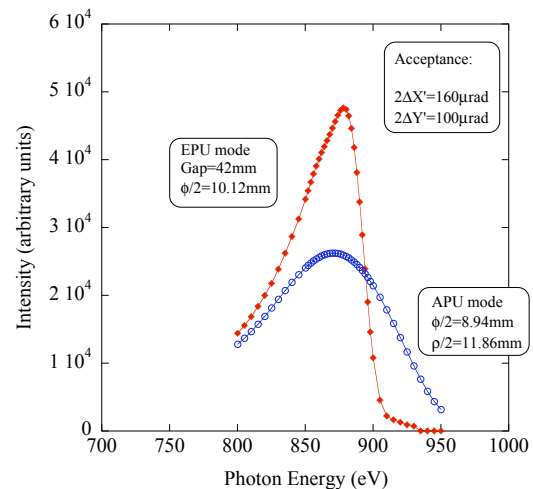


Figure 10  
Obtained spectra of the circular polarization for the APU and EPU modes.



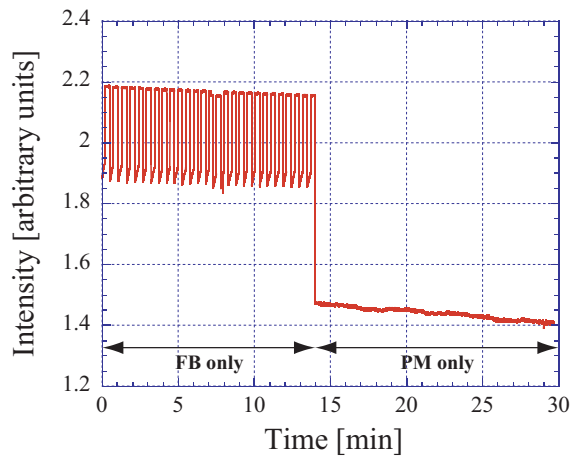


Figure 13  
Time evolution of the SR intensity at BL-17. “FB” and “PM” indicate bunch-by-bunch feedback and RF phase modulation, respectively. The SR intensity was measured by with an ionization chamber.

Our future problem is to realize stable and high-intensity SR with the bunch-by-bunch feedback system alone. The best way to do so is to identify and improve the impedance sources that excite the quadrupole-mode instabilities. We are designing a feedback system dedicated to the suppression of quadrupole-mode oscillations for cases in which it is difficult to identify the impedance sources.

## REFERENCES

- [1] *Photon Factory Activity Report 2006*, **24A** (2008) 106.
- [2] *Photon Factory Activity Report 2007*, **25A** (2009) 114.
- [3] S. Sakanaka, M. Izawa, T. Mitsuhashi and T. Takahashi, *Phys. Rev. ST Accel. Beams*, **3** (2000) 050701.
- [4] D. Teytelman, C. Rivetta, D. Van Winkle, R. Akre, J. Fox, A. Krasnykh, A. Drago, J. Flanagan, T. Naito and M. Tobiya, *EPAC 2006*, (2006) 3038

## 2-5 Test of a Hybrid Fill Mode

The time structure of synchrotron radiation (SR) emitted from an electron storage ring depends on the pattern of filled RF buckets. The fill pattern can be roughly classified into two types: multibunch and single-bunch patterns. Although a PF ring is usually operated in the multibunch mode with 280 bunches, it is sometimes operated in the single-bunch mode at a user’s request for pulsed SR. A hybrid fill mode is a compromise between these two operation modes. This mode consists of a train of low-current bunches and a single high-current bunch. This popular mode has been adopted as one of the user operation modes in large storage rings such as ESRF and SPring-8 [1, 2]. However, it has not yet been tested in the PF ring with a relatively higher revolution frequency than ESRF and SPring-8. At the request of single-bunch users, we carried out a feasibility study on the hybrid fill mode in October 2008.

The test experiment was performed in two steps. First, we injected the beam into a series of buckets corresponding to one half of the ring (156 buckets) until the stored current reached 400 mA. Then, we injected the beam into a bucket located at the middle of the other half for the stored current of up to 450 mA and achieved the hybrid fill pattern, as shown in Fig. 14. However, during this procedure, bunch-by-bunch feedback system is not available because of the high contrast of currents between the bunch train and the single bunch. Therefore, in this experiment, we suppressed multibunch instabilities in the transverse and longitudinal planes by using the octupole magnets and RF phase modulation, respectively. We also suppressed single-bunch instabilities by controlling ring chromaticity. All procedures were performed carefully while monitoring the beam profile and vacuum pressure at various points around the ring in order to avoid critical heat generation caused by unexpected beam losses.

Figures 15 (a) and (b) are the fill patterns and beam spectra observed before and after the injection of the single bunch. The fill patterns and beam spectra were measured by a wall-current monitor and a button-type pickup electrode, respectively. We observed that the beam spectrum changes to a flat distribution peculiar to the single-bunch mode upon injection of the high-current single bunch into the opposite side of the bunch train. Figure 16 shows the ratio of vacuum pressures in the hybrid fill mode to that in the typical multibunch mode (280 bunches, 450 mA) plotted against the address of the ring components. For comparison, the result of the typical single-bunch mode (50 mA) has been superposed on it. The positions where the vacuum was degraded due to local heat generations are not fully consistent; however, the distribution of vacuum pressures along the ring and the rate of vacuum degradation are similar for the hybrid fill and the typical single-bunch mode. Figure 17 shows the fill pattern in the hybrid fill mode obtained by using a streak camera. In this case, the pulse width of SR emitted from the single-bunch component is estimated to be around 100 ps.

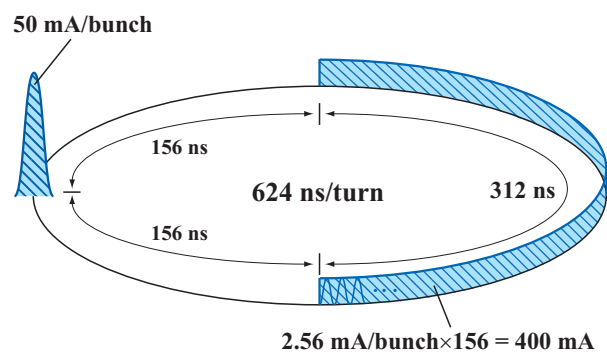
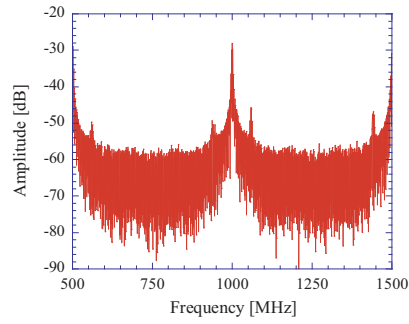
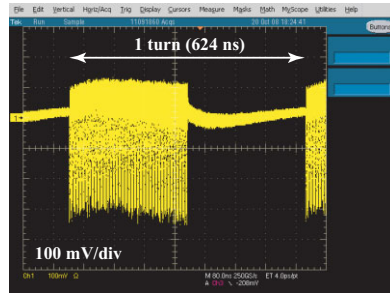


Figure 14  
Schematic representation of the tested fill pattern. Total current is 450 mA.



(a) without single bunch



(b) with single bunch (Hybrid fill)

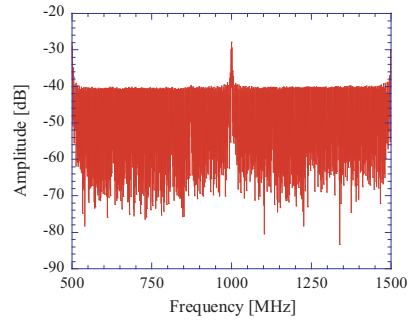
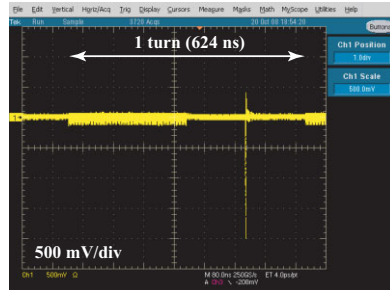


Figure 15  
Fill patterns and beam spectra observed before and after the injection of the single bunch.

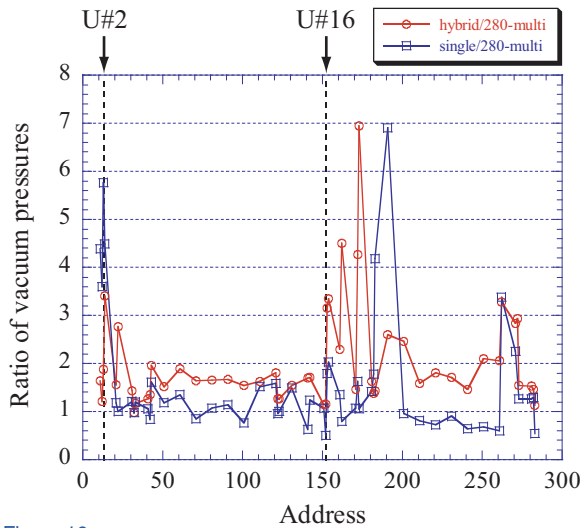


Figure 16  
Comparison between the distributions of vacuum degradation along the ring in the hybrid fill and typical single-bunch mode.

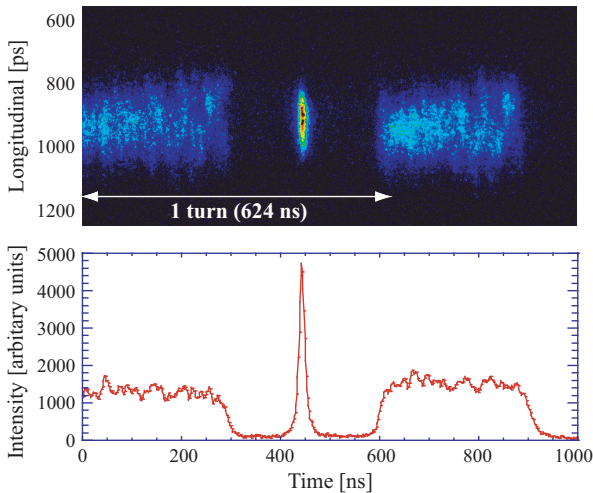


Figure 17  
Fill pattern in the hybrid fill mode obtained by using a streak camera.

Thus, we successfully stored a 450-mA current by means of the hybrid fill mode: 1/2 filling (2.56 mA/bunch  $\times$  156) + 1 single bunch opposite to the bunch train (50 mA/bunch). To adopt the hybrid fill mode in user operations at the PF ring, we have to solve the following technical problems:

- Top-up injection for the single-bunch component with a short lifetime.
- Cleaning of the front and rear of the single-bunch component (Bunch purification).
- Selective application of bunch-by-bunch feedback to the multibunch component.
- Measurement of lifetime and current for each component.

REFERENCES

[1] J. M. Filhol, L. Hardy and U. Weinrich, *PAC 1999*, (1999) 2334.  
 [2] T. Nakamura, T. Fujita, K. Fukami, K. Kobayashi, C. Mitsuda, M. Oishi, S. Sasaki, M. Shoji, K. Soutome, M. Takao, Y. Taniuchi and Z. Zhou, *EPAC 08*, (2008) 3284.

## 2-6 Stored Beam Stability during Pulsed Sextupole Injection

To suppress stored beam oscillation during beam injection for synchrotron radiation (SR) sources, we proposed a beam injection system using a pulsed sextupole magnet (PSM) [1, 2] and installed it at the PF ring in the spring of 2008. The beam injection with the PSM system was successfully operated [3] and the electron beam up to 450 mA, regular operating beam current of the PF ring, could be stored using this system.

The advantage of the PSM injection is that the beam oscillation of the stored beam during the injection can be very small. We compared the stored beam oscillation in the PSM injection with that in the bumped orbit injection using a turn-by-turn beam position monitor (BPM). The stored beam oscillation was measured in the single-bunch mode to monitor it precisely and the stored beam current was set to around 10 mA. Figure 18 shows the horizontal and vertical beam dipole oscillations. During the bumped orbit injection, large dipole oscillations in both the horizontal and vertical directions were observed as shown in Figs. 18 (c) and (d). The oscillations were generated due to the leakage of the bumped orbit formed with four pulsed kicker magnets. The amplitudes of the oscillations were about 850  $\mu\text{m}$  for the horizontal direction and 130  $\mu\text{m}$  for the vertical direction at the maximum. On the other hand, as shown in Figs. 18 (a) and (b), the amplitudes during PSM injection were reduced to about 180  $\mu\text{m}$  in the horizontal direction and 40  $\mu\text{m}$  in the vertical direction. The amplitude of the vertical oscillation with the PSM injection corresponds to almost the noise level of the turn-by-turn BPM system.

The dipole oscillations of the stored beam in the PSM injection were sufficiently reduced, compared with those in the bumped orbit injection. In particular, such small vertical oscillation allows high-quality SR experiments even during the injection.

To show that the PSM top-up injection is also effective for high-quality SR experiments, we measured the stability of photon intensity at BL-14A. The operating mode of the PF ring was a multi-bunch mode and the top-up beam current was 450 mA. The both injection systems, the PSM injection and the bumped orbit injection, were fired at 1 Hz without an injected beam, so as to monitor the effect on the stored beam directly. The effect of the injected beam on the photon intensity is estimated 2~3% in the top-up injection from the ratio of the number of particles in the injected beam to the stored beam, slightly depending on the injection conditions.

BL-14A has a vertical superconducting wiggler and its photon intensity stability is very sensitive to the horizontal beam oscillation during beam injection. The photon intensity was measured with an ionization chamber and a PIN photodiode after focusing by a toroidal mirror and passing through a pinhole of 0.8 mm diameter. In Fig. 19, the black line is an output signal of the PIN photodiode. If the photon intensity during the beam injection is constant, the signal from the ionization chamber and the photodiode has a constant value of around unity. However, the photon intensity had a 1 Hz spike train, which exactly synchronized with the beam injection. For the bumped orbit injection, the maximum change of the photon intensity was very large, about 70%. On the other hand, it became only 1~2% with the PSM injection. This result shows that the PSM injection is very effective for the top-up injection.

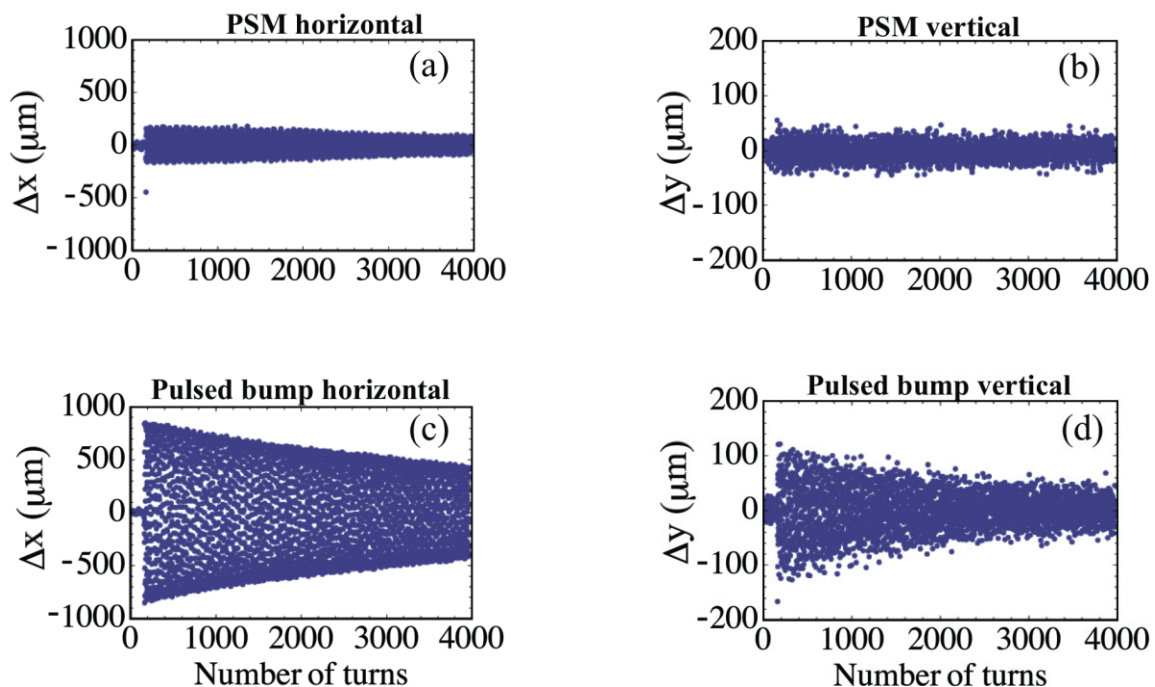


Figure 18

Horizontal and vertical beam oscillations ( $\Delta x$  and  $\Delta y$ ) of the stored beam immediately after the beam injection. The oscillations produced by the PSM injection are shown in the upper two figures, (a) and (b), and those by the bumped orbit injection are in the lower two figures, (c) and (d).

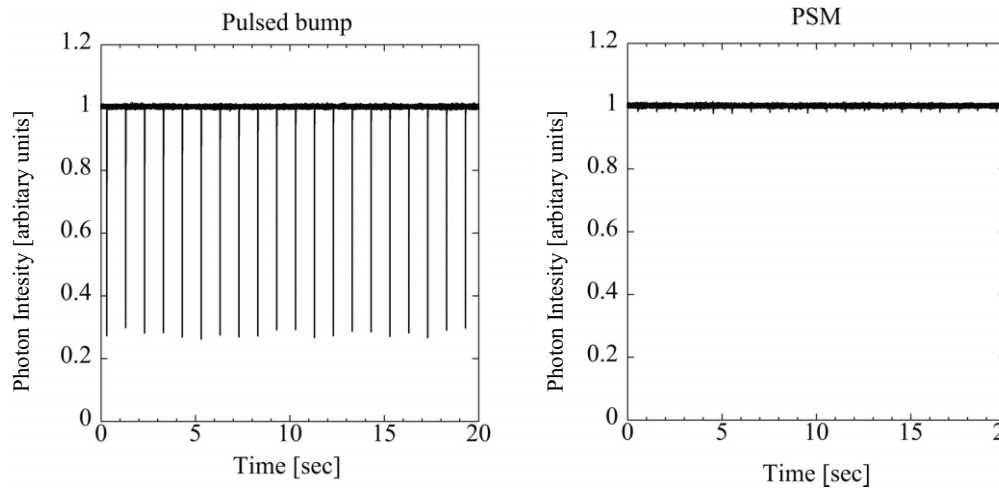


Figure 19 Stability of photon intensity at BL-14A in the pulsed bumped orbit injection (left graph) and the PSM injection (right graph). The spike appeared at exactly 1 Hz in both graphs. The sampling rate of the signals is 10 kHz.

In summary, we measured the stored beam oscillation and the photon intensity during top-up operation comparing the PSM injection with the bumped orbit injection at the PF ring. By changing the injection scheme from the pulsed bump injection to the PSM injection, the maximum amplitude of dipole oscillation of the stored beam was reduced from  $850\ \mu\text{m}$  to  $180\ \mu\text{m}$  in the horizontal direction and from  $130\ \mu\text{m}$  to  $40\ \mu\text{m}$  in the vertical direction. The photon intensity fluctuation at BL-14A during the top-up injection was also stabilized from 70% to 1~2% at maximum. We confirmed that the stability of the stored beam during the injection was improved by the PSM compared with the conventional bumped orbit scheme at the PF ring.

## REFERENCES

- [1] Y. Kobayashi and K. Harada, *Proc. of EPAC 2006*, (2006) 3526.
- [2] H. Takaki, N. Nakamura, Y. Kobayashi, K. Harada, T. Honda, T. Miyajima and S. Nagahashi, *Proc. of PAC 2007*, (2007) 230.
- [3] H. Takaki, N. Nakamura, K. Harada, T. Honda, Y. Kobayashi, T. Miyajima, S. Nagahashi, T. Obina and A. Ueda, *Proc. of EPAC 2008*, (2008) 2204.